Subsonic Stability and Control Characteristics of Configurations Incorporating Wrap-Around Surfaces

E. F. Lucero*
Applied Physics Laboratory, The Johns Hopkins University, Laurel, Md.

The aerodynamic feasibility of using wrap-around lifting, stabilizing, and controlling surfaces on tube-launched bank-to-turn missile configurations is established by wind tunnel tests at high subsonic speeds. Test results show that the stability and control characteristics of a wrap-around-surface configuration are as good or better than those of an equivalent planar-surface configuration. Predictions based on planar surfaces agree well with test results when surface-to-surface interference is not present. An improved prediction method for tail efficiency of wrap-around-surface configurations is shown. Several configurational design preferences are indicated by the test results, including: a high wing (concave side windward) to a low wing (convex side windward); horizontal tails mounted with their concave side windward when in the undeflected position; and a windward directional stabilizer. From all observatiions on the aerodynamic effectiveness of wrap-around-surfaces, a configuration having *all* of its surfaces wrap-around appears to be aerodynamically feasible.

Nomenclature

C_ℓ = rolling moment coefficient, rolling moment/qSd
C_m = pitching moment coefficient, pitching moment/qSd, about $X/\ell_B = 0.55$
C_n = yawing moment coefficient, yawing moment/qSd, about $X/\ell_B = 0.55$
C_N = normal force coefficient, normal force/qS
d = body diameter, 3.0 in.
$h_{t(\text{eff})}$ = effective tail height for wrap-around surface, Fig. 10
i_p = pitch control-surface deflection, Table 1
i_Y = yaw (directional) control-surface deflection, Table 1
ℓ_B = body length, 30 in.
M = Mach number
MAC = mean aerodynamic chord
q_ℓ, q_∞ = local and freestream dynamic pressure, respectively
S = reference area, $S = \pi d^2/4$
X = body longitudinal station, measured rearward from nose tip
C_{F_α} = $\partial C_F/\partial\alpha$ at $\alpha = 0$, where $F = m, N$
C_{F_β} = $\partial C_F/\partial\beta$ at $\beta = 0$, where $F = \ell, n$
C_{ℓ_δ} = roll control effectiveness obtained from $\Delta C_\ell/\delta$
ΔC_F = increment in C_F, where $F = \ell, m, n, N$ resulting from the deflection of control surfaces
α_H = local angle-of-attack at the ¼ chord point of the MAC of the horizontal tail
α_R = resultant angle-of-attack, $\alpha_R = \alpha$ as used in C_{F_α}
α_{mi} = α_R at maximum wing-tail interference
β = angle-of-sideslip
δ = average differential tail deflection, Table 1
$\bar{\epsilon}$ = average downwash angle at the ¼ chord point of the MAC of the horizontal tail, $\bar{\epsilon}$ is positive in direction of $-\alpha_R$
η_{HV} = tail efficiency in providing longitudinal stability
$d\bar{\epsilon}/d\alpha$ = change in $\bar{\epsilon}$ with α_R

Nomenclature of Model Parts

B = body alone consisting of a von Karman nose of fineness ratio *2.1* followed by a cylindrical afterbody of fineness ratio *7.9*
H_C = wrap-around horizontal tail, concave to windward at $+\alpha_R$, $i_p = 0$
H_P = planar horizontal tail
W_C = wrap-around wing, concave to windward at $+\alpha_R$
W_P = planar wing
V_I = planar vertical tail located windward at $+\alpha_R$

Introduction

RECENT interest in tube-type launching systems leads naturally to consideration of configurations with foldable or wrap-around lifting surfaces which fit compactly into such launchers and also provide satisfactory aerodynamic performance. In the stowed position these surfaces would be folded so as to fit within a circular cylinder defined by the maximum diameter of the missile body.

The present study has concentrated on the use of wrap-around surfaces in order to maximize the volume available in the missile. Most of the previous interest in wrap-around surfaces has been in their application as stabilizing fins on bombs and projectiles,[1-6] thus previous investigations have considered only spirally oriented fins having essentially constant thickness profiles. The specific application prompting the present study would be in a high-subsonic missile using a bank-to-turn control system.

The objective of the experiments reported in this paper was to assess the aerodynamic feasibility of a configuration using wrap-around wings and wrap-around stabilizing and control surfaces. Corollary objectives were to evaluate the relative effectiveness of wrap-around and planar surfaces having subsonic profiles, and to determine the adequacy of predictive methods based on planar surfaces for preliminary design of wrap-around surfaces.

Description of the Experiments

Models

The wrap-around surface configuration consisted of a fineness ratio 10 body upon which were mounted wrap-around wings, wrap-around horizontal tails, and a planar vertical tail (Fig. 1). The body had a 2.1 caliber von Karman nose followed by a cylindrical afterbody. Since drag optimization was not a primary goal in the design or test, the body was not contoured nor boattailed. The wings were elevated 30° from

Received June 16, 1976; presented as Paper 76-366 at the AIAA 9th Fluid and Plasma Dynomics Conference, San Diego, Calif., July 14-16, 1976; revision received Aug. 30, 1976. This study was supported by NAVSEA-035. The author gratefully acknowledges the guidance provided in this investigation by L.L. Cronvich and E.T. Marley.

Index categories: LV/M Aerodynamics; LV/M Configurational Design.

*Engineer, Fluid Dynamics Group. Member AIAA.

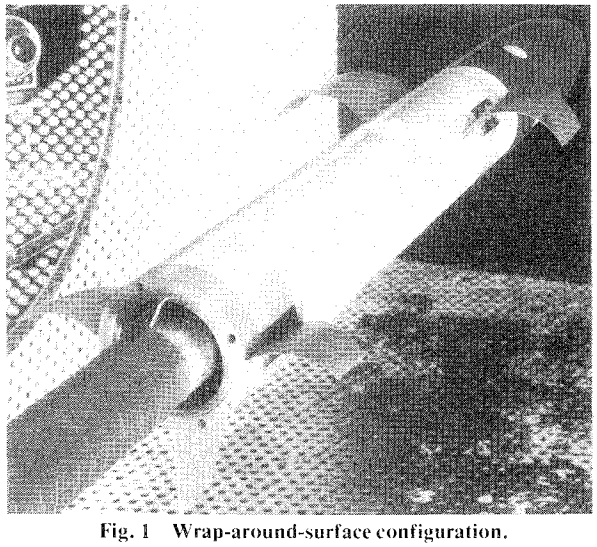

Fig. 1 Wrap-around-surface configuration.

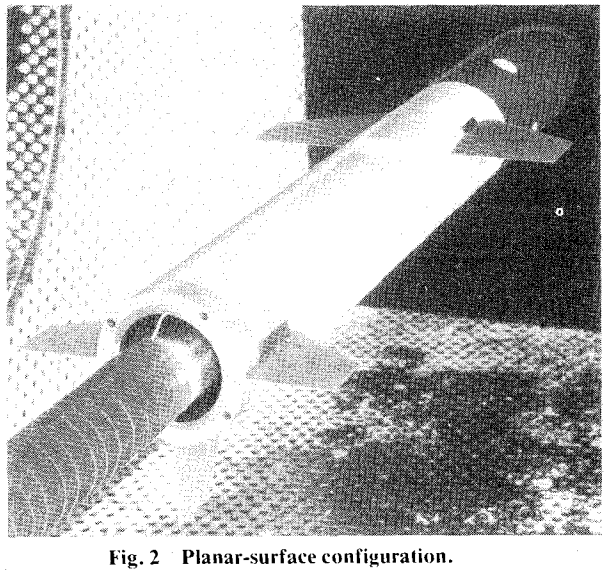

Fig. 2 Planar-surface configuration.

Table 1 Geometric parameters of wing and tail surfaces

PARAMETERS[a]	WING	HORIZONTAL TAIL	VERTICAL TAIL
EXPOSED SEMI-SPAN, IN.	2.598	1.760	1.760
ROOT CHORD, IN.	3.737	2.514	2.514
TIP CHORD, IN.	1.868	1.257	1.257
MEAN AERO. CHORD, IN.	2.907	1.956	1.956
PROJECTED SURFACE AREA (ONE SURFACE) IN^2	7.281	3.318	3.318
TAPER IN CHORD	1/2	1/2	1/2
SWEEP, DEG. (REF.)	35.6°	35.6°	35.6°
ASPECT RATIO, ONE EXPOSED PANEL	0.927	0.933	0.933
SECTION PROFILE: NACA 64A006 ALL SURFACES			

CONTROL SURFACE DEFLECTIONS (LOOKING UPSTREAM)

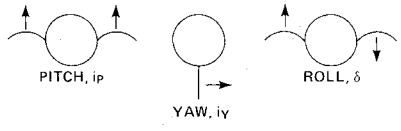

(ARROWS POINT TO DIRECTION OF DEFLECTION OF LEADING EDGE)

[a] NOTE: FOR THE WRAP-AROUND SURFACE THESE GEOMETRIC PARAMETERS REFER TO THE PROJECTION OF THE WRAP-AROUND SURFACE ON THE HORIZONTAL PLANE CONTAINING BOTH THE ROOT AND TIP CHORDS.

the horizontal plane of the cylinder to obtain the maximum wing span when unfolded without requiring overlap when folded. The horizontal tails, which were mounted on the midplane of the body, were tested at nominal pitch control deflections of 0°, ±5°, and ±10° and at roll control deflections of 5° and 10°. The vertical stabilizer was tested at yaw control deflections of 0° and 10°. The profile of all the surfaces was NACA 64A006 and the planform was trapezoidal with a taper ratio of ½. The exposed aspect ratio was 1.85 for two surfaces. This profile and this planform were selected partly on the basis of their favorable drag divergence and stall characteristics.[7,8] The planform was also selected to obtain a combination of aspect ratio and area which optimizes the product of normal force coefficient slope and planform area.

Configurations similar to the wrap-around-surface configuration but with planar surfaces (Fig. 2) were also tested for comparison. These surfaces had the same planform as the projected planform of the wrap-around surfaces. Other geometric parameters for the test models are given in Table 1.

A limited amount of testing was conducted with other configurational variables including: a wrap-around vertical tail; horizontal tail concavity orientation, dihedral, and anhedral; and wing longitudinal position. The ¼ chord point of the mean aerodynamic chord of the wing is at 60% of the body length for the longitudinal stability characteristics reported herein, and for the control and lateral stability characteristics it is a 50% of the body length.

Test Conditions and Procedures

Aerodynamic normal and side forces and pitching, yawing, and rolling moments were obtained in the General Dynamics/Convair Transonic wind tunnel mostly at $M=0.8$.[9] A limited amount of data were also obtained at $0.65 \leq M \leq 0.98$. The freestream Reynolds number was 7.5×10^6 per foot. The angle of attack was varied from $-12°$ to 16°. This variation in α_R provided information on both high and low wing configurations and on the surface concavity effects (concave or convex). Sideslip effects were obtained at $\alpha_R = 0°, 6°$, and 12°.

Results of Wind Tunnel Tests

Longitudinal Stability

Wing-Body

No significant difference was observed between the C_N (or C_m) data of the wrap-around wing-body and planar wing-body configurations when the wing is high (concave surface windward), Figs. 3 and 4; the body-low wing (convex surface windward) is slightly less stable than the high wing configuration at $\alpha_R \gtrsim 6°$. Within the accuracy indicated by the data, reasonable engineering estimates can be obtained using planar surface methods provided that the projected planforms are the same for the planar and wrap-around wings. For example, the method of Polhamus[10] (although derived for fully tapered wings) in conjunction with slender body interferences factors[11] gives a good prediction of wing normal force coefficient plus mutual body-wing interference (Fig. 5). (Lamar's more general method[12] obtains for cropped deltas values of the viscous contribution to lift that are within 10% of Polhamus' values for delta wings.) Lifting surface theory[13] was found to accurately predict the slope of C_N vs α_R at $\alpha_R = 0$. For center-of-pressure estimates, test data indicate that the ¼ chord point of the mean aerodynamic chord would be a reasonable engineering estimate in the Mach number and angle of attack range tested.

Tail-Body

A similar comparison of the tail-body data also shows little difference between the longitudinal stability characteristics of the wrap-around and the planar tails which have the same planform, although wrap-around tails provide slightly more stability at high positive angle of attack.

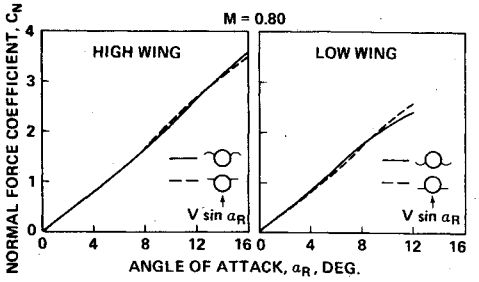

Fig. 3 Normal force coefficient (wing-body configurations).

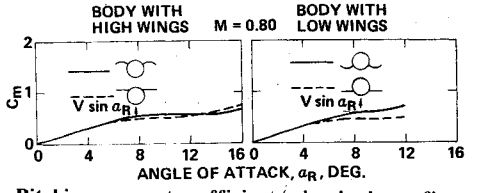

Fig. 4 Pitching moment coefficient (wing-body configurations).

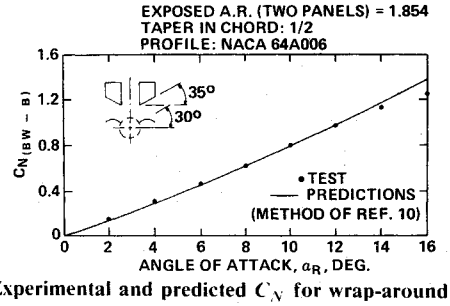

Fig. 5 Experimental and predicted C_N for wrap-around wings plus wing-body carryover.

Body-Wing-Tail Configuration Data

The full configuration (body-wing-tail) using wrap-around surfaces has essentially the same value of C_N as the full configuration using planar surfaces up to $\alpha_R \approx 12°$ when the wing is high and up to $\alpha_R \approx 8°$ when the wing is low (Fig. 6); the stability of the wrap-around configuration is equal to or higher (C_m more negative) than the stability of the planar-surface configuration (Fig. 7) when the wing is high. The low-wing (concave side leeward) wrap-around configuration is much less satisfactory than the high-wing (concave side windward) wrap-around configuration in that at a given α_R it has a lower value of C_N (Fig. 8) and less longitudinal stability. Thus, in the most likely operating range of angle of attack (positive α_R) the wrap-around-surface configuration with the high wing is more aerodynamically desirable than either the wrap-around-surface configuration with the low wing or the configuration which has all planar surfaces.

Efficiency of Tails for Longitudinal Stabilization

When the horizontal tail stabilizer is in the presence of the wing wake, its stabilizing effectiveness is reduced because of the wing downwash. The ratio of the pitching moment contribution from the tail with the wing present to that obtained when the wing is not present is the tail efficiency, η_{HV}. A comparison of this parameter for the wrap-around- and planar-surface configurations shows (Fig. 9) that the tails of the wrap-around-surface configuration are more efficient stabilizers than the tails of the planar-surface configuration. The experimental data from the wrap-around-surface configuration are compared in Fig. 10 with a) the values of η_{HV} calculated using Decker's downwash formulation derived for planar surfaces,[14] i.e.

$$\eta_{HV} = q_t/q_\infty\,[1 - (d\bar{\epsilon}/d\alpha)]$$

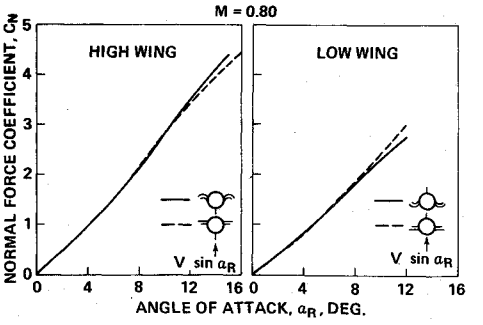

Fig. 6 Normal force coefficient (full configurations).

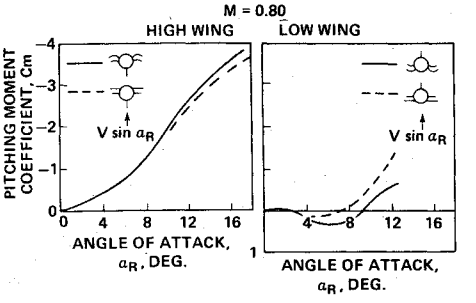

Fig. 7 Pitching moment coefficient (full configurations).

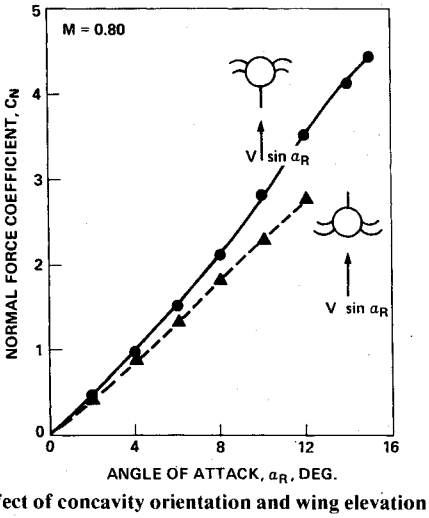

Fig. 8 Effect of concavity orientation and wing elevation on C_N.

and b) with the same formulation of $d\bar{\epsilon}/d\alpha$ but modified by an effective tail height parameter, $h_{t(\mathrm{eff})}$, based on the geometry of the wrap-around surfaces (see sketch of Fig. 10). An improvement in the predicted value of η_{HV} for the wrap-around-surface configuration is obtained when $h_{t(\mathrm{eff})}$ is used. The use of this effective tail height in Decker's downwash formulation also provided, for other wrap-around-surface configurations investigated in this study) a good prediction of the angle at which the wing vortex cores cross the tails (angle of maximum interference, α_{mi}) (Table 2).

Longitudinal Control

Longitudinal control is obtained by deflection of the horizontal tails. Tests were conducted with positive and negative control surface deflections, i_p. The actual fabricated values of i_p are indicated in Fig. 11. When the wrap-around tails are deflected to negative values of i_p, i.e., convex side windward at $\alpha_R = 0$, the magnitude of the control moment per degree of control surface deflection, $\Delta C_m/i_p$, is generally greater than that of the planar tails (Fig. 11). When the wrap-around tails are deflected to positive values of i_p, i.e., concave side wind-

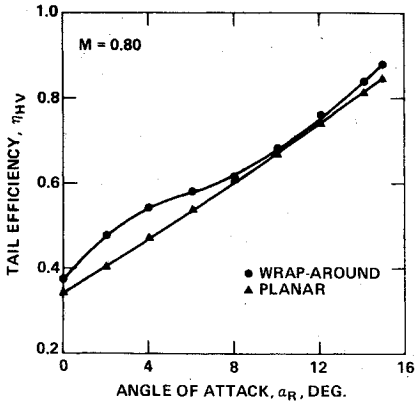

Fig. 9 Tail efficiency, experimental.

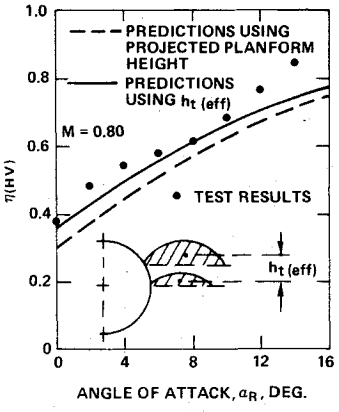

Fig. 10 Comparison of experimental and predicted η_{HV} of wrap-around-surface configuration.

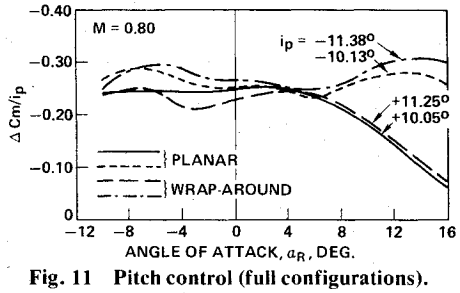

Fig. 11 Pitch control (full configurations).

ward, the magnitude of $\Delta C_m/i_p$ is generally less than that of the planar tails. When the convex side of the wrap-around tails is windward, a larger control moment is obtained than when the concave side is windward. This situation is desirable since (for steady state conditions) a stable missile would normally be maneuvering with a negative value of control surface deflection. Thus for the expected operating range of angle of attack and control surface deflection for a stable bank-to-turn missile, the wrap-arouind tails have a pitch control effectiveness that is generally greater than that of the planar tails.

The data on control effectiveness for both wrap-around-surface and planar-surface configurations correlates as almost a single valued function of the local tail angle-of-attack, α_H, (Fig. 12) for both body-tail and body-wing-tail configurations. It is therefore suggested that, for a given body-wing-tail configuration having wrap-around surfaces, the control effectiveness parameter $\Delta C_m/i_p$, can be obtained empirically from a plot of $\Delta C_m/i_p$ vs α_H obtained from the data from a body-tail configuration. The applicable value of α_H for the body-wing-tail configuration is obtained from α_H

Table 2 Comparison of α_{mi} with predictions using $h_{t(\text{eff})}$

CONFIGURATION	$h_{t(\text{eff})}$, in.	α(mi), DEG. TEST	PREDICTED
BODY-LOW WING CONVEX SIDE WINDWARD WITH TAIL:			
CONCAVE WWD AND 30° ANHEDRAL	0.805	4.2	5.6
CONVEX WWD, 0° DIHEDRAL	0.983	6.2	6.9
PLANAR TAIL, 0° DIHEDRAL	1.125	7.0	7.8
CONCAVE WWD, 0° DIHEDRAL	1.267	7.8	8.9
CONVEX WWD, 30° DIHEDRAL	1.451	10.3	10.2

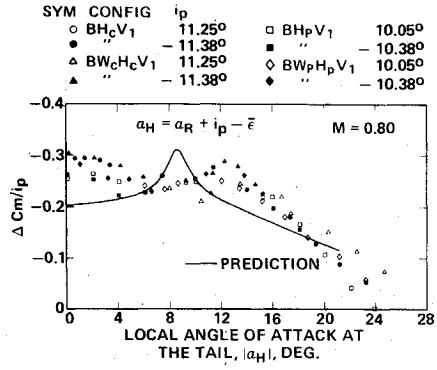

Fig. 12 Correlation of $\Delta C_m/i_p$ with α_H.

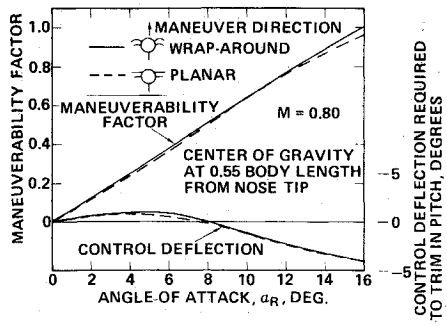

Fig. 13 Longitudinal trim characteristics.

$=\alpha_R + i_p - \epsilon$. The average downwash angle of ϵ is calculated using the proper value of $h_{t(\text{eff})}$ for the given wrap-around-surface configuration as depicted by Fig. 10. In the absence of body-tail data, predictive methods derived for planar surfaces provide a reasonable estimate of $\Delta C_m/i_p$ for preliminary design (see curve of Fig. 12). The predicted values shown in Fig. 12 were calculated using the leading-edge suction analogy[10] with account made for tail-body interference by using slender body interference factors.[11] Note that ΔC_m is the difference between the value of C_m at $i_p \neq 0$ and the value of C_m at $i_p = 0$. The predicted value of $\Delta C_m/i_p$ is generally lower than the present data and thus provides a conservative value of $\Delta C_m/i_p$.

Longitudinal Trim Characteristics

The trim maneuverability and control characteristics for a center-of-gravity position at 55% of the body length are shown in Fig. 13 for both wrap-around-surface and planar-surface configurations. These results are for configurations whose ¼ chord point of the MAC of the wing is at $0.50\ell_B$. Trim indicates that the sum of the moments is zero. The maneuverability factor shown in Fig. 13 is the trim value of C_N at a given angle of attack normalized by the trim value of C_N for the wrap-around configuration at an angle-of-attack of 16°. Note that the wrap-around-surface configuration has a maneuver capability that is slightly greater than that of the planar-surface configuration. The tail control deflections

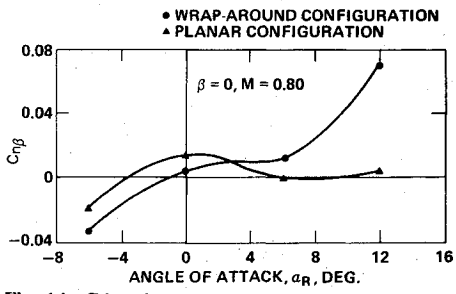

Fig. 14 Directional stability (full configurations).

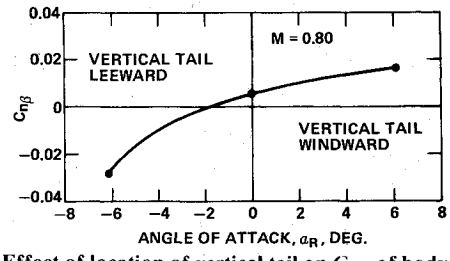

Fig. 15 Effect of location of vertical tail on C_{n_β} of body-vertical tail configuration.

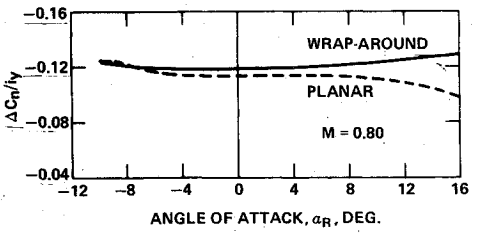

Fig. 16 Directional control (full configurations).

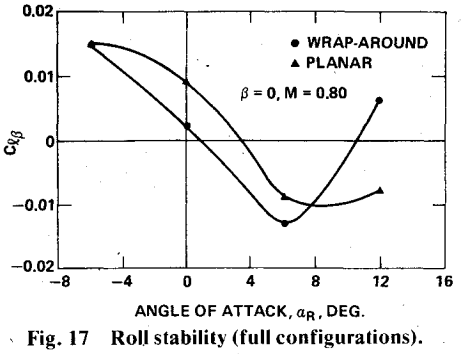

Fig. 17 Roll stability (full configurations).

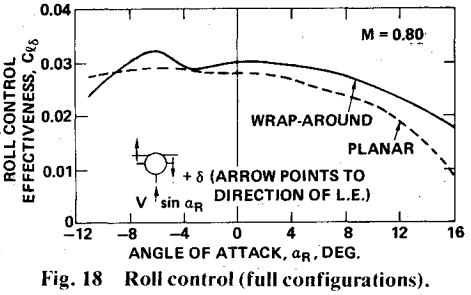

Fig. 18 Roll control (full configurations).

needed to hold either the wrap-around- or planar-surface configuration at the desired angle of attack are less than |5°|. Thus the wrap-around-surface configuration is aerodynamically feasible from the standpoint of longitudinal trim characteristics.

Directional Stability

The wrap-around surface configuration has directional stability characteristics that are generally more favorable (i.e., more stable) than those of the planar-surface configurations in the expected operating regime, although both appear to be satisfactory (Fig. 14).

An important result obtained from the component data is that the effectiveness of the vertical stabilizer in providing directional stability is significantly reduced when it is located in the leeward flow (Fig. 15). Thus the windward location for a vertical stabilizer is more desirable than the leeward location.

A single run at $\alpha_R = 0$ on a configuration consisting of a body and wrap-around vertical tail showed that the wrap-around vertical tail provided more than twice the directional stability, C_{n_β}, of the planar vertical tail. These results are in consonance with the linearized (about $\alpha_R = 0$) longitudinal stability characteristics which showed that the wrap-around tails (wings) had higher values of C_{N_α} and C_{m_α} than the planar wings. The small increment in lift due to curvature (directed towards the center of curvature at subsonic speeds) observed by Featherstone,[3] and others, may be the reason for these differences.

Directional Control

The directional control effectiveness of a planar vertical panel at $\beta = 0$ is slightly higher when used with the wrap-around-surface configuration than when used with a planar-surface configuration and neither is affected greatly by angle of attack (Fig. 16). The effect of slideslip on directional control effectiveness (at a given angle of attack) was found to be small.

Roll Stability

The roll stability of both the wrap-around- and planar-surface configurations increases with angle of attack (i.e., C_{l_β} becomes more negative) up to $\alpha_R \approx 8°$ (Fig. 17). The wrap-around-surface configuration is more stable in roll than the planar-surface confiuration for angles of attack up to 8°. Sideslip data at $\alpha_R = 0°$ from the wing-body configurations showed that the wrap-around wings produce 1.6 times more roll stability than the planar wings.

At $\alpha_R \gtrsim 8°$, the wrap-around-surface configuration exhibits decreasing roll stability and becomes unstable in roll at $\alpha_R \approx 11°$. The source for this decreasing roll stability could not be determined from the data available. This roll instability of the wrap-around-surface configuration exhibited at $\alpha_R > 11.2°$ should not present any problems in controlling the missile. The results of simple calculations of control surface deflections required to trim in pitch, yaw and roll for maneuvers at $\alpha_R = 12.7°$ verify this.

Roll Control

The roll control effectiveness, C_{l_δ}, of the wrap-around tails is equal to or better than that of the planar tails (Fig. 18). At $\alpha_R > 0$, C_{l_δ} decreases with increasing α_R for the wrap-around tails but not as much as it does with the planar tails. The reduction of C_{l_δ} with α_R is due to the onset of stall of the left panel at $\alpha_H \approx 12°$ (see Fig. 12). The importance of this reduced value of C_{l_δ} at the higher angles of attack on aerodynamic performance depends on potential mission requirements.

Control Surface Interactions

Limited investigations were conducted to determine the extent of control surface interactions when the controls are deflected in combination. The interaction of the yaw control on pitch control and vice-versa were found to be negligible.

The induced roll resulting from yaw control, $\Delta C_l/i_Y$, is somewhat lower for the wrap-around than for the planar-

surface configuration even though the yaw control panel is planar for both configurations. The test results indicate that the reason for this is that the interference from the wrap-around horizontal tails but not from the planar tails, reduces the magnitude of $\Delta C_l/i_Y$; neither the wrap-around nor planar wings have any significant effect on $\Delta C_l/i_Y$ for $\alpha \leq 10°$. The sideslip angle β has only a slight effect on the yaw-induced rolling moment $\Delta C_l/i_Y$.

A yawing moment is induced when the horizontal panels are deflected for roll control. This induced yawing moment, $\Delta C_n/\delta$, is essentially the same for the wrap-around- and planar-surface configurations, and is affected more by angle of attack than by sideslip angle.

Conclusions

The use of wrap-around surfaces for providing lift, stability, and control of span limited missiles is aerodynamically feasible. The aerodynamic characteristics of the wrap-around surfaces can be predicted satisfactorily for preliminary design using methods developed for planar surfaces. For body-wing-tail configurations, where wing-tail interference is present, an effective tail height parameter has been developed in this study for wrap-around-surface configurations that can be used to obtain reasonable predictions of tail efficiency.

References

[1] Gauzza, H. J., "Static Stability Test of Tangent and Wrap-Around Fin Configurations at Supersonic Speeds," U. S. Naval Ordnance Laboratory, White Oak, Md., NAVORD Report 3743, Jan. 17, 1955.

[2] Wells, R. F., "Investigation of the Aerodynamic Characteristics of a Model of a Rocket Missile with Several Arrangements of Folding Fins at Mach Numbers of 1.75, 2.15, 2.48 and 2.87," NASA TMX-234, April 1960.

[3] Featherstone, H.A., "The Aerodynamic Characteristics of Curved Tail Fins," General Dynamics/Pomona, Calif., GDC-ERR-PO-019, Sept. 1960.

[4] Regan, F. J. and Schermerhorn, V. L., "Supersonic Magnus Measurements of the 10-Caliber Army-Navy Spinner Projectile with Wrap-Around Fins," U. S. Naval Ordnance Laboratory, White Oak, Md., NOLTR 70-211, Oct. 1, 1970.

[5] Craft, J. C. and Skorupski, J., "Static Aerodynamic Stability Characteristics of Munitions Designs at Transonic Mach Numbers," USAMC, Redstone, Arsenal, Ala., RD-73-3, Feb. 1973.

[6] Dahlke, C. W. and Craft, J. C., "Aerodynamic Characteristics of Wrap Around Fins Mounted on Bodies of Revolution and Their Influence on Missile Static Stability at Mach Numbers from 0.3 to 1.3," USAMC, Redstone Arsenal, Ala, RD-TM-72-1, Vol. I, March 1972 and Vol. II, April 1972.

[7] Daley, B. N. and Dick, R. S., "Effect of Thickness, Camber and Thickness Distribution on Airfoil Characteristics at Mach Numbers up to 1.0," NACA TN 3607, March 1956.

[8] Allen, E. C., "Experimental Investigations of the Effects of Planform Taper on the Aerodynamic Characteristics of Symmetrical Unswept Wings of Varying Aspect Ratio," NACA RM A53C19, May 29, 1953.

[9] General Dynamics/Convair Division, "High-Speed Wind Tunnel Facility Manual," San Diego, Calif., Oct. 1969.

[10] Polhamus, E. C., "Predictions of Vortex-Lift Characteristics by a Leading Edge Suction Analogy," *Journal of Aircraft*, Vol. 8, April 1971, pp. 193–199.

[11] Pitts, W. C., Nielsen, J. N. and Kaattari, G. E., "Lift and Center-of-Pressure of Wing-Body-Tail Combinations at Subsonic, Transonic, and Supersonic Speeds," NACA Report 1307, 1957.

[12] Lamar, J. E., "Extension of the Leading-Edge Suction Analogy to Wings With Separated Flow Around the Side Edges at Subsonic Speeds," NASA TR-R-428, Oct. 1974.

[13] Diederich, F.W., "A Planform Parameter for Correlating Certain Aerodynamic Characteristics of Swept Wings," NACA TN 2335, April 1951.

[14] Decker, J. L., "Prediction of Downwash at Various Angles of Attack for Arbitrary Tail Locations," *Aeronautical Engineering Review*, Vol. 15, Aug. 1956, pp. 22–27, 61.